Green and Stable Processing of Organic Light-Emitting Diodes from Aqueous Nanodispersion

*Anielen Halda Ribeiro, Ahmed Fakih, Bas van der Zee, Lothar Veith, Gunnar Glaser, Alexander Kunz, Katharina Landfester, Paul W. M. Blom, Jasper J. Michels**

ELECTRONIC SUPPLEMENTARY INFORMATION (ESI)

S1. SEM analysis PPV:PS nanoparticles films on glass-Au-PEDOT:PSS and glass-ITO-PEDOT:PSS

Figure S1 shows spin-cast films of SY-PPV:polystyrene nanoparticles, spin-coated in three consecutive passes onto a) glass-gold-PEDOT:PSS and b) glass-ITO-PEDOT:PSS substrates. Each coating pass is preceded by a mild substrate pretreatment using a nitrogen plasma (see Experimental section in the main document).

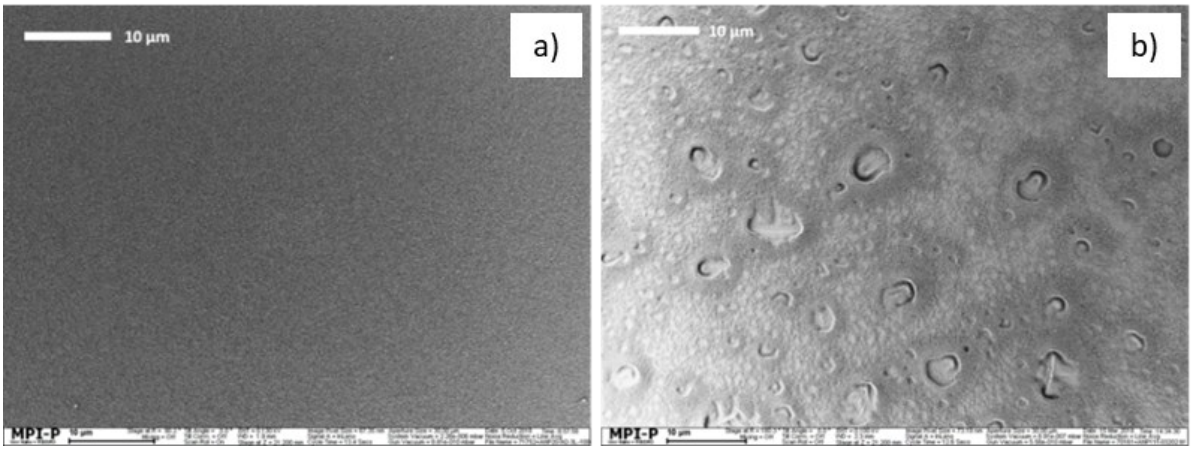

Fig. S1. *SY-PPV:polystyrene nanoparticle films on a) glass-Au-PEDOT:PSS and b) glass-ITO-PEDOT:PSS, each obtained after three consecutive spin-coating passes.*

S2. ToF-SIMS analysis

Figure S2 shows the raw ToF-SIMS traces recorded using an IONTOF TOF.SIMS NCS with 30 keV Bi_3^+ primary ions for the nanoparticle-MEH-PPV:PS-PEDOT:PSS stack shown in Figure 4 of the main document. The panels show the traces of the positive (2a) and negative (2b) ions plotted as a function of the number of scans. The traces have been obtained by sputtering the organic stack with 5 keV Ar_{1500} cluster ions above the glass area of the substrate (*i.e.* a region not covered by gold). Since for the glass-gold substrates the inorganic interface does not affect the film formation (see above), measuring above glass or gold is expected to give a similar result. In Table S1 the detected monovalent ions have been assigned as fragments originating from various species present in the organic stack. The fact that the steep decline in the intensity of PPV- and PS-related ions coincides with a steep rise in intensity of the PSS-related fragments supports the presence of a well-defined interface between the

PPV:PS nanoparticle-rich and PEDOT:PSS-rich regions. Upon reaching the glass surface the intensity of silicon-containing ions rises with a concomitant decline in the PSS-related signals. We have indicated the PPV:PS-rich and PEDOT:PSS-rich regions with yellow and blue shades, the substrate being indicated in grey.

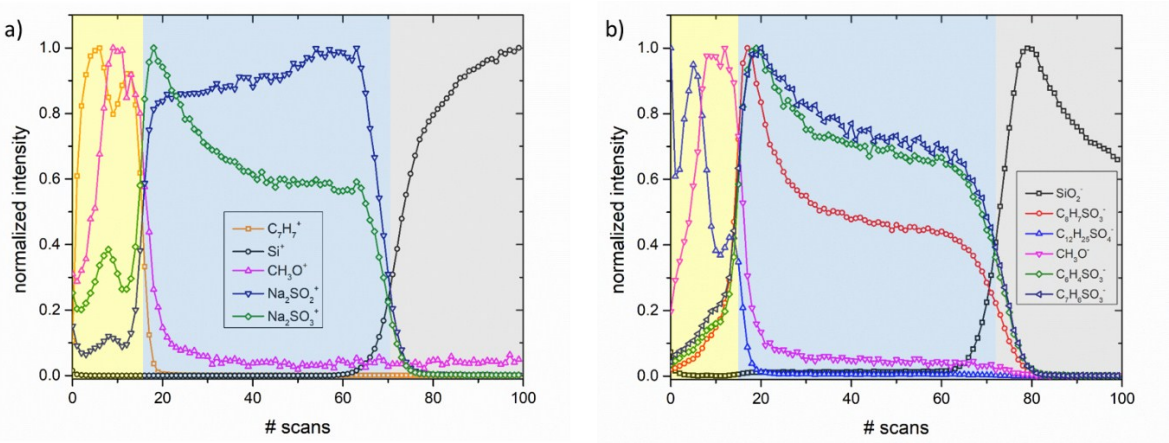

Fig. S2. *Raw ToF-SIMS traces recorded for the nanoparticle-MEH-PPV:PS-PEDOT:PSS stack. The traces have been plotted as normalized ion intensities as a function of the number of scans. Panels a) and b) respectively show the traces for the positive and negative ions. The colored boxes indicate the MEH-PPV:PS-rich/PEDOT:PSS-poor region (yellow), the MEH-PPV:PS-poor/PEDOT:PSS-rich region (blue) and the (glass) substrate (grey).*

Table S1. *Assignment of ionic fragments detected during ToF-SIMS on the nanoparticle-MEH-PPV:polystyrene-PEDOT:PSS stack.*

cation	source	anion	source
$C_7H_7^+$	polystyrene	SiO_2^-	glass (substrate)
Si^+	glass (substrate)	$C_8H_7SO_3^-$	PSS
CH_3O^+	MEH-PPV	$C_{12}H_{25}SO_4^-$	SDS (molecular ion)
$Na_2SO_2^+$	PSS	CH_3O^-	MEH-PPV
$Na_2SO_3^+$	PSS	$C_6H_4SO_3^-$	PSS
		$C_7H_6SO_3^-$	PSS

Due to a difference in the sputter rates between the different materials, the widths of the shaded regions do not represent an actual physical thickness. In order to be able to convert the number of scans into thickness estimates, we independently determined the sputter rates of PPV:PS (1:1) and PEDOT:PSS on separate films with known thickness. Films of 77 nm PPV:PS (solution-cast) and 56 nm

PEDOT:PSS required 43 s and 145 s, respectively, for full removal. This corresponds to sputter rates of $k_1 = 1.8$ and $k_2 = 0.4$ nm/s, respectively. With these values we estimate the thickness of the PPV:PS-rich and the PEDOT:PSS-rich regions using the following relation:

$$d_{i=1,2} \approx L k_i N_i \left(k_1 N_1 + k_2 N_2\right)^{-1} \quad \text{(S1)}$$

Here, d_i denotes the thickness of the PPV:PS-rich ($i = 1$) and PEDOT:PSS-rich ($i = 2$) layers, L is the total thickness of the combined organic stack (measured by profilometry to be L = 140 nm) and N_i represents the number of scans required to sputter through the PPV:PS-rich and PEDOT:PSS-rich regions ($N_1 \approx 18$ and $N_2 \approx 52$). Plugging these values into Equation S1 gives: $d_1 \approx 85$ nm and $d_2 \approx 55$ nm.

S3. Transmittance Au-anode

Figure S3 shows the transmittance spectrum we record for of a 20 nm gold layer on top of a glass substrate. We observe that in the spectral range of the SY emission, the transmittance is roughly ~30%, which is about a factor three lower than for ITO, which exhibits a transmittance of ~90% in the same spectral region. To allow for comparison with values obtained for OLED devices based on (the more commonly) used ITO-anodes, we multiply the measured current efficiencies by a factor 3.

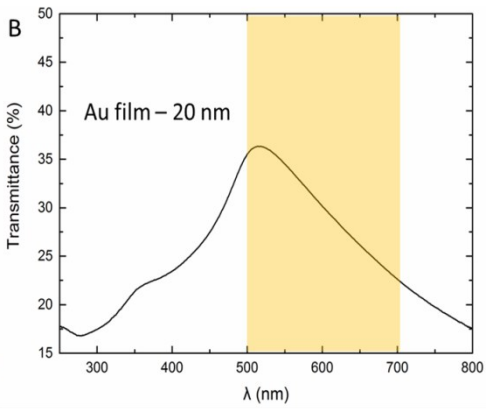

Fig. S3. *UV-Vis transmittance spectrum of a thermally evaporated layer of 1 nm layer of chromium followed by 20 nm gold on a glass substrate. The yellow area indicates the spectral range of the SY emission.*

S4. Polystyrene-free nanoparticle OLEDs

In order to demonstrate the necessity of the blending of the PPV with polystyrene in order to achieve optimal device performance, we fabricated reference devices with active layers processed from nanodispersion of the pure MEH-PPV. We determined the particle size at: 64±16 nm. SEM analysis of these films seem to reveal a higher density of holes and defects in comparison to the films processed from PPV:PS particles (see Figure S4 in comparison to Figure S1). Consequently, PLEDs processed from the aqueous MEH-PPV nanodispersion, with a ~60 nm active layer following the same two-pass casting procedure that we used for the MEH-PPV:PS dispersion, generally exhibit a significantly enhanced leakage current (see Figure S5) as compared to both the MEH-PPV:PS nanoparticle- and reference devices (see main document Figure 7a).

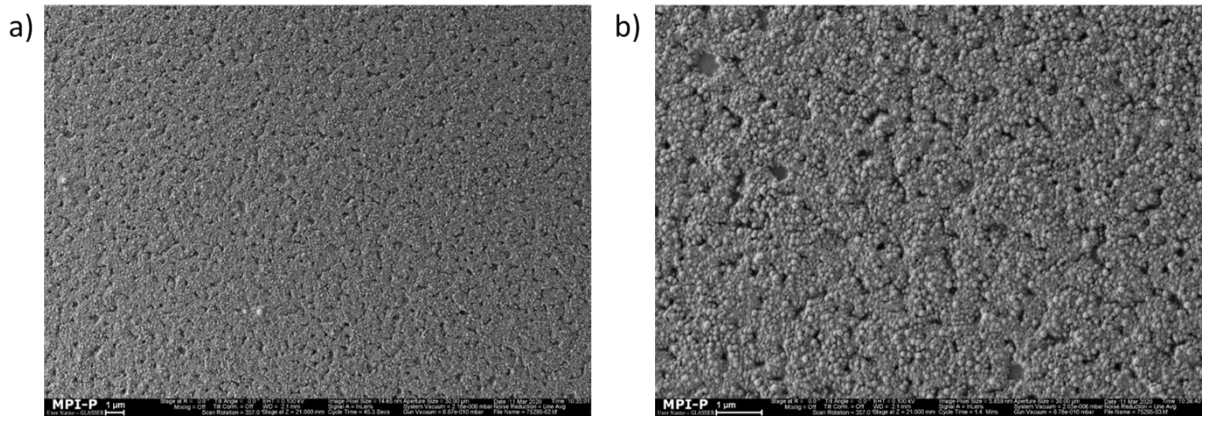

Fig. S4. *SEM topview images of an MEH-PPV nanoparticle film cast in two passes onto PEDOT:PSS and annealed for 2h at 110 °C.*

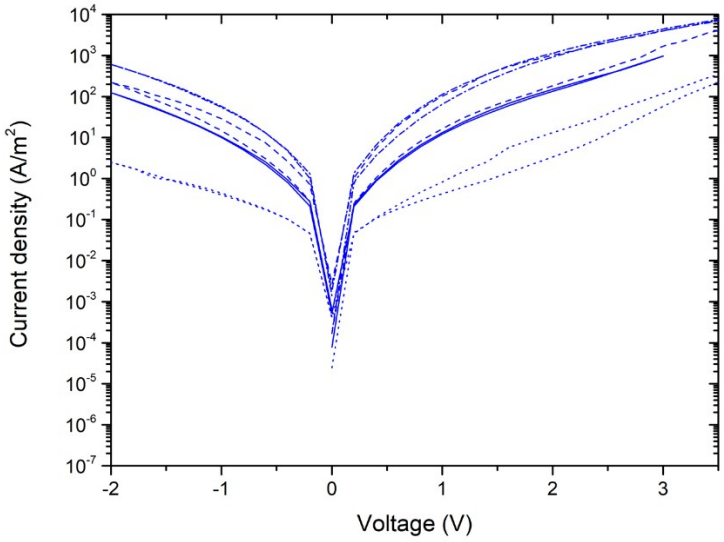

Fig. S5. *Current density plotted as function of voltage, recorded for various PLED devices with an MEH-PPV nanoparticle active layer. Each line type represents a different device.*

In Figure S6 we integrated the JVL and luminous efficiency of the best performing MEH-PPV nanoparticle device, *i.e.* the one with the lowest leakage current, with Figure 7 of the main document. The figure reveals that even for this device the leakage current (blue curve) is still an order of magnitude higher than for the MEH-PPV:PS nanoparticle (red) and solution-cast (black) devices. This may partly explain the lower efficiency of the MEH-PPV nanoparticle device in comparison to the MEH-PPV:PS nanoparticle device. Besides, the fact that the active layer of the former is significantly lower than the optimum of ~90 nm (with ideal optical cavity), an additional loss may be expected due to reduced light outcoupling.[1]

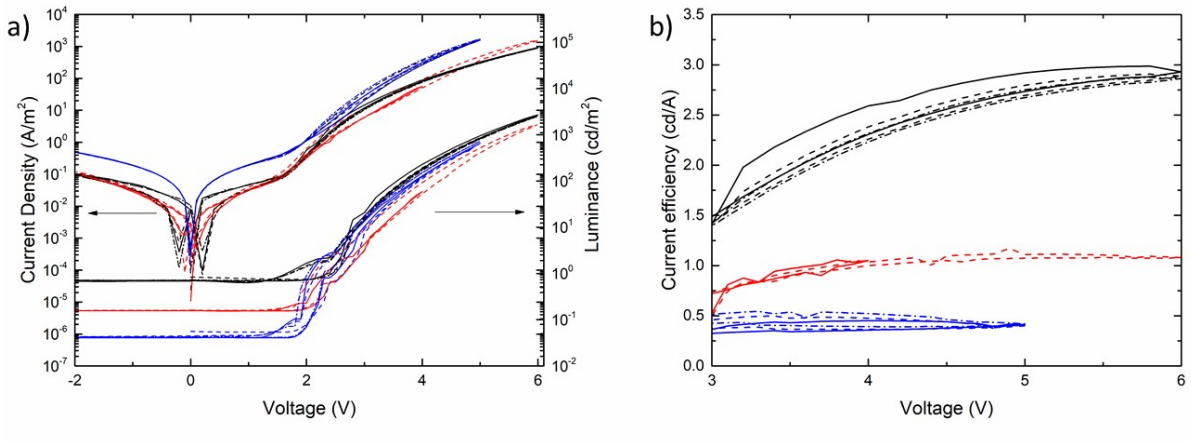

Fig. S6. *(a) Current density (J) (left y-axis) and luminance (right y-axis), plotted as a function of applied voltage (V) for an MEH-PPV:PS nanoparticle PLED with an 85 nm active layer (red), an MEH-PPV nanoparticle PLED with a 60 nm active layer and a solution-cast MEH-PPV:PS reference device with a 90 nm active layer (black). (b) Current efficiencies of the MEH-PPV:polystyrene, MEH-PPV nanoparticle (red, blue) and reference (black) devices, plotted as a function of voltage. Solid, dashed and dash-dotted lines represent consecutive voltage scans. All curves have been measured at 295 K.*

1. D. Abbaszadeh, N. Y. Doumona, G. A. H. Wetzelaer, L. J. A. Koster, P. W. M. Blom, *Synth. Met.*, 2016, **215**, 64-67.